Chapter 6
Gradient Art: Creation and Vectorization

Pascal Barla and Adrien Bousseau

Abstract There are two different categories of methods for producing vector gradients. One is mainly interested in converting existing photographs into *dense* vector representations. By vector it is meant that one can zoom infinitely inside images, and that control values do not have to lie onto a grid but must represent subtle color gradients found in input images. The other category is tailored to the creation of images from scratch, using a *sparse* set of vector primitives. In this case, we still have the infinite zoom property, but also an advanced model of how space should be filled in-between primitives, since there is no input photograph to rely on. These two categories are actually extreme cases, and seem to exclude each other: a dense representation is difficult to manipulate, especially when one wants to modify topology; a sparse representation is hardly adapted to photo vectorization, especially in the presence of texture. Very few methods lie in the middle, and the ones that do require user assistance. The challenge is worth the effort though: it would make converting an image into vector primitives easily amenable to stylization.

6.1 Introduction

Among existing methods employed to create stylized images, drawing is the oldest one. The notion of *style* is complex though, and goes from the tools and medium used to produce an image, to rules of image composition. The focus of this chapter is on *color gradients*, that form a basic, yet essential part of style in digital drawing.

Pascal Barla
Inria Bordeaux, 351, cours de la Libération, 33405 Talence cedex, e-mail: `pascal.barla@inria.fr`

Adrien Bousseau
Inria Sophia Antipolis, 2004 route des Lucioles, 06902 Sophia Antipolis Cedex, France e-mail: `adrien.bousseau@inria.fr`

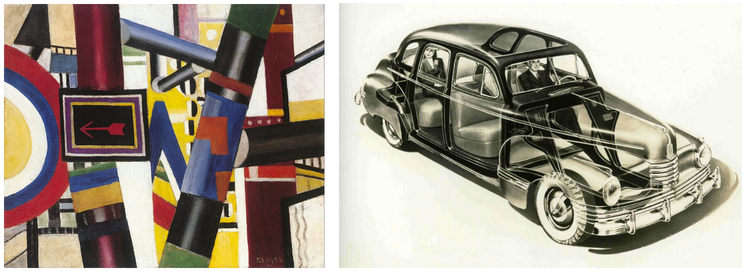

(a) Fernand Leger (b) Nash Ambassador

Fig. 6.1 Smooth color gradients are ubiquitous in art and illustration.

Examples of color gradients abound in paintings, as well as in illustrations and graphic novels. Although such pictures may make use of very different media such as watercolor, oil paint, acrylic or pencil, they all tend to reproduce gradients in similar respects. Firstly, they are not constrained by physical accuracy: a few smooth gradients are enough to produce a convincing appearance or to elicit a feeling through an abstract composition. Second, they exhibit sharp color discontinuities that may be used to convey occluding edges or to create shading or stylization effects. Compositions made of color gradients may be obtained in different ways: by carefully reproducing the gradients found in a photograph, by freely taking inspiration and then departing from them, or by being directly drawn from scratch. In this chapter, we consider the whole spectrum of techniques to create color gradients in digital images.

Before starting our investigation of computer-aided methods for the drawing of color gradients, let us take a brief look at hand-made paintings and drawings and how they use these gradients. In pure color compositions such as abstract art (see Fig. 1.1a), gradients may convey an abstract sense of motion or lighting. The level of abstraction varies among artists, and for that reason there is no a priori family of gradients that could be made to answer every imaginable artistic needs. Other compositions make use of smooth shading-like gradients to convey characters and objects in a rather iconic style, like in the art of Tamara de Lempicka. Although her style is a lot more figurative, it is still quite far from an accurate reproduction of a real-world image: in particular, shapes and lighting are often drastically simplified. In industrial design, communication imperatives make the use of color gradients more tightly coupled with faithful shape reproduction (see Fig. 1.1b). However, industrial designers often depart from realistic shading to convey shape and materials unambiguously. Even hyper-realistic images make use of color gradients in their own specific way. Although such images look surprisingly similar to photographs, they actually go further than photo-realism by showing details that could not be seen with the naked eye, thus exaggerating the impression of realism.

When it comes to *digital* drawing in general, and color gradients in particular, one is faced with a choice between two alternatives: either use raster or vector graphics.

Raster graphics solutions such as Adobe Photoshop, Corel Painter or Gimp offer by design a more direct analogy with traditional, hand-made paintings and drawings: each drawn brush stroke is recorded in a pixel grid that represents the canvas, and blended in a variety of ways depending on the choice of tool and medium. Tools may tightly simulate their real-world counterparts (e.g., [2]), or they might provide novel types of interactions (e.g., [18]). In both cases though, users create color gradients by layering multiple strokes. The first issue raised by this layering approach is that the resulting gradient is not easily editable, and artists usually have to re-paint over them when a change is required. A second limitation of raster images is their lack of scalability: the resolution of the pixel grid limits the amount of details that can be drawn.

Vector graphics, on the other hand, offer a more compact representation, resolution independence (allowing scaling of images while retaining sharp edges), and geometric editability. Vector-based images are more easily animated (through keyframe animation of their underlying geometric primitives), and more readily stylized (e.g. through controlled perturbation of geometry). For all of these reasons, vector-based drawing tools, such as Adobe Illustrator, Corel Draw, and Inkscape, continue to enjoy great popularity, as do standardized vector representations, such as Flash and SVG.

However, for all of their benefits, *basic* vector drawing tools offer limited support for representing complex color gradients, which are integral to many artistic styles. In order to better understand these limitations, let us consider the following two important requirements for any vector-based solution:

1. Accurate manual control should be provided at sharp discontinuities, while a somewhat more automated control (albeit accurate) is preferable in smooth regions. These different levels of control are necessary because small changes of sharp color variations are more noticeable, while smooth color variations are more difficult to draw.
2. Completing a drawing should require as few vector primitives as possible to get to the intended result. Such sparse representations are necessary to endow artists with more direct control of entire parts of the image at once, and limit the amount of user interaction for simple edits.

Basic color gradient tools have huge restrictions regarding both requirements. In a nutshell, they require many primitives to create even simple images, work solely with closed contours, and provide only for very simple interior behaviors. Section 1.2 explains these limitations in detail, and presents the alternative primitives that form the core of this chapter.

Despite considerable improvements in vector-based color gradient primitives, we must say that as of today, there is no single solution that fulfils the above-mentioned requirements unequivocally. This is mainly due to the extent to which each method makes use of a reference raster image. For methods that strive to faithfully convert a photograph to a vector representation — a process known as vectorization — primitives need to stick as much as possible to underlying color variations (req.1), hence making it hard to provide holistic editing functionalities (req.2). On the opposite end of the spectrum, methods that let artists create color gradients from scratch — i.e., vector drawing — must at the same time provide control in precise locations (req.1), and incorporate priors to fill-in smooth regions with few primitives (req.2). These examples are extreme cases, and a host of intermediate solutions has been proposed in the literature. This is elaborated in greater depth in Section 1.3.

An ideal solution would reside in a single tool for both vector drawing and image vectorization: one could start from an image and more or less deviate from it according to the intended message conveyed by the picture, in a style either personal or optimized for legibility for instance. Even if such a method becomes available one day, there will still be a last important point to consider: with more advanced conversion and editing capabilities come more complex rendering requirements. To reach a wide audience, the rendering of vector-based color gradients should be efficient (ideally real-time) and robust (artifact-free). We present in Section 1.4 existing rendering solutions and compare their merits.

The gradient primitives, construction techniques and rendering algorithms presented in the following sections have been used for applications outside of color gradients. One important instance is the (re-)construction of normal and/or depth images (e.g. [14]), which provide for 3D-like shading capabilities. We refer the interested reader to Sections 12.3.2 to 12.3.3 of this book, where it is shown how diffusion-based methods in particular have proven useful for a variety of applications. We have intentionally focused on still 2D graphics; throughout the chapter, we will also mention vector-based 3D methods, but only in contexts where they are of interest to 2D color gradients.

6.2 Gradient primitives

We start by describing existing gradient primitives, focusing on how they are created and manipulated. We distinguish between three families of primitives: elemental primitives that fill the whole space given a small set of parameters, primitives that rely on meshes to provide more accurate and dense control, and primitives that rely on extremal curves and a propagation process to fill-in space between them.

6.2.1 Elemental gradients

Elemental gradients are composed of two ingredients: a parametrization of the plane $\mathbb{R}^2 \rightarrow [0,1]$, and a one-dimensional color gradient $[0,1] \rightarrow [0,1]^4$ that assigns a color and opacity to each parametric value. The types of gradients differ in the way they define the parametrization from two control points. The most common parametrizations are linear, radial and polar, as shown in Fig. 1.2: a linear gradient produces constant colors along directions perpendicular to the line defined by the two control

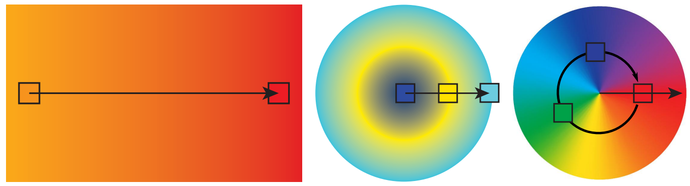

(a) Linear (b) Radial (c) Polar

Fig. 6.2 Examples of elemental gradients and their parameterization and color control points.

points; a radial gradient produces circles of constant colors centered on the first control point; a polar gradient produces rays of constant colors originating from the first anchor point. In the last case, the 1D gradient should be periodic to avoid color discontinuities. The distance function may be adapted to produce contours of constant colors with different shapes, such as rectangles or stars.

Each gradient is controlled by a pair of 2D control points (at least) for the parametrization, and a series of colors and opacity control values arranged on the $[0,1]$ interval. A piecewise-linear interpolation is commonly used to define this 1D color function, although other interpolants such as splines can produce smoother variations. The final 2D color gradient is either assigned to the background, or to the interior of a closed 2D shape.

While the extent of an elemental gradient can be infinite, these primitives are often used to fill-in closed shapes. Figure 1.3(a) shows a complex image created entirely with linear and radial gradients. Figure 1.3(b) highlights how a linear gradient fills a region to produce a convincing reflection. Although this example is compelling, it requires advanced skills and a lot of time to complete a drawing. This is why elemental gradients are most of the time confined to simple compositions.

6.2.2 Gradient meshes

The main idea of a gradient mesh is to decompose the image plane into a connected set of simple 2D patches $P_i : \mathbb{R}^2 \rightarrow [0,1]^2$, and assign each patch a color based on a *two-dimensional* color gradient $[0,1]^2 \rightarrow [0,1]^4$. It improves on the elemental

(a) Complex combination of gradients (b) Individual linear gradient

Fig. 6.3 Complex images require the combination of a multitude of elemental gradients.

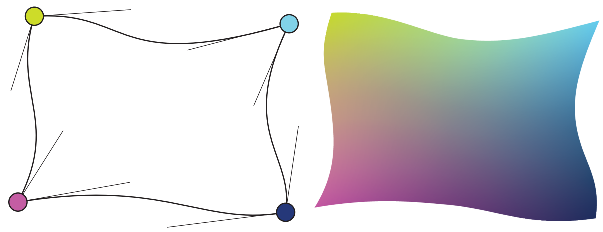

(a) Control points and tangents (b) Interpolated colors

Fig. 6.4 Example of a simple gradient mesh.

gradients in two ways: the mesh structure permits gradient structures to be produced that are a lot more complex; and the use of a 2D elemental gradient for each patch permits a greater variety of smooth color variations to be created.

The original gradient mesh tool is based on quad patches with curved boundaries, as illustrated in Figure 1.4. RGB colors and tangents are assigned to each vertex of the mesh. Colors are interpolated inside the patch guided by tangents, which allows artists to finely tune color variations inside a patch.

This tool provides a far more advanced control over the structure of the gradients: any kind of curve can be used. However, the grid-like structure constrains the topology of control curves as a whole: users must align the main direction of the quad mesh with the structure of the drawing they want to create in advance, and holes are not easily treated. In practice, two types of grid are commonly employed: Cartesian and angular grids. Their use depends on the structure of the gradient to be drawn, which must often be decided in advance as well.

Alternative representations for gradient meshes have been proposed, such as the triangular patches of Xia et al. [25]. Although in most cases colors are stored at vertices and interpolated over patches [21, 22], some methods store color control points inside the patches [25]. Such representations are more adapted to image vectorization, as will be discussed in Section 1.3.

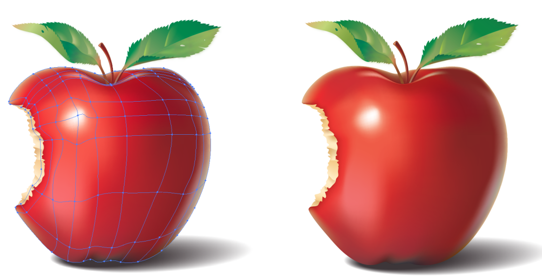

(a) Dense gradient mesh (b) Interpolated colors

Fig. 6.5 Gradient meshes are well suited to represent the smooth shading and subsurface scattering of organic materials.

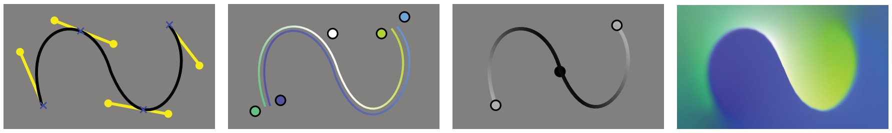

(a) Geometry (b) Color (c) Blur (d) Final image

Fig. 6.6 A Diffusion curve is composed of (a) a geometric curve described by a Bézier spline, (b) arbitrary colors on either side, linearly interpolated along the curve, (c) a blur amount linearly interpolated along the curve. The ïňĄnal image (d) is obtained by diffusion and reblurring. Note the complex color distribution and blur variation defined with a handful of controls.

Figure 1.5 shows a Cartesian gradient mesh used to depict an apple. Note how the structure has to be bent around the highlight, and the density of lines increased near silhouettes. Gradient meshes are quite similar in spirit to 3D meshes, with which artists have learnt to represent a shape with the smallest number of patches; except that gradient meshes represent 2D color gradients instead of 3D surfaces.

The use of gradient meshes thus not only provides a gain in accuracy, but also increases the number of control points that must be manipulated by the artist to reach a desired goal, and requires some experience to make the right choice of structure in advance.

6.2.3 Gradient extrema

The idea of using extrema (i.e. discontinuities) of color gradients to represent images originally comes from the Vision literature. Among the many papers that have stressed their importance, Elder's article [7] has insisted on the ability of edges to encode most of the visual information in an image.

Following this work, Diffusion Curves [19] have been introduced as a vector-drawing primitive entirely based on extremal curves of color gradients. A primitive path consists of a Bézier curve $C_i : [0,1] \to \mathbb{R}^2$ to which is assigned color control points on either side of the curve. Colors are first interpolated along the curve to yield two 1D color gradients $[0,1] \to [0,1]^3$, one for each side of the curve; second, colors are extrapolated to the whole image plane through a propagation process, which mimics heat diffusion in the original approach. The primitive may be augmented with blur control points, located anywhere on the curve. They are also interpolated along the curve to yield a single blur gradient $[0,1] \to [0,1]$, which is then used to control the sharpness of the color transition from one side to the other. This is illustrated in Figure 1.6.

The main advantage of this primitive compared to others is that it leaves artists free to position extremal curves anywhere they want and to vary their number depending on the amount of detail they wish to depict. Gradient extrema do not have to be closed and nearby curves interact together more than curves that are far apart. They may also intersect, although care should be taken with color assignment in this

(a) Diffusion Curves (b) Interpolated colors

Fig. 6.7 Diffusion Curves can represent freeform color gradients such as the folds in this stylized cloth.

case: the presence of multiple colors at the location of the intersection will produce visual artifacts. Proper user interfaces remain to be proposed to facilitate color assignment in such configurations. The ability to blur color transitions across curves allows artists to create interesting effects without having to duplicate primitives or to adjust their color control points, as it is the case with gradient meshes.

The main limitation of diffusion curves is the lack of control over the propagation of colors. This is the reason why several extensions have been proposed to improve artistic control using directional diffusion and blockers [3, 4], or to produce a smoother color propagation [10]. Jeschke et al. [13] also use diffusion curves to control the parameters of procedural textures, while Hnaidi et al. [11] create height fields by diffusing height from curves that represent ridges and cliffs. Finally, Takayama et al. [24] extend diffusion curves to diffusion surfaces to create volumetric models with 3D color gradients.

Figure 1.7 shows a drawing made using diffusion curves. The complex fold patterns would have been difficult to obtain with a more structured primitive such as a gradient mesh. It is also natural to add more curves to increase details with this approach. On the downside, the method is less localized than gradient meshes: for instance, to obtain the black background colors, it is necessary to assign black colors outside of all contour curves. This is partly solved by the use of Diffusion Barriers [3], but an efficient treatment of occluding contours and layers remains an open research challenge.

6.3 Construction techniques

There is an obvious visual gap between the primitives illustrated in Figs. 1.2, 1.4 and 1.6 and the complex drawings obtained with them, shown in Figs. 1.3, 1.5 and 1.7. With enough skill and patience, these latter images may be drawn man-

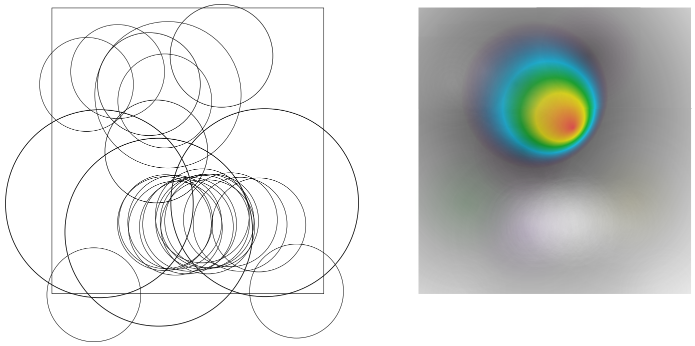

(a) Combination of radial gradients (b) Complex color variations

Fig. 6.8 Multiple elemental (here radial) gradients (a) need to be combined to create more complex color variations (b).

ually from scratch. However, an often faster solution is to take an input photograph as a reference, either by using the image to guide the drawing process, or by relying on a conversion algorithm that involves no intervention on the part of the artist.

6.3.1 Manual creation

Elemental gradients are often assigned to their own layer or 2D shape and blended with layers below. With this approach, a lot of blended primitives are required to obtain color gradients that are not directly expressible from available elemental primitives, as shown in Figure 1.8.

When working with gradient meshes, artists first need to indicate the number of meshes necessary to represent each part of the drawing. Then, as with 3D modelling tools, artists often start with a low resolution and add in details progressively. With a

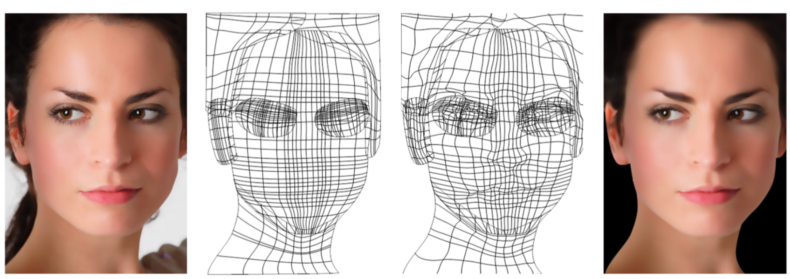

(a) Input bitmap (b) Initial gradient mesh (c) Optimized gradient mesh (d) Resulting image

Fig. 6.9 Starting from a user-defined mesh (b), Sun et al. [22] optimize the position and color of the vertices (c) to best match an input bitmap (a,d). ©Copyright 2007 ACM.

regular quad-based mesh, users can add vertical or horizontal curves, move control points and assign them new colors. Finer meshes are often needed to draw objects with complex topology.

When a reference image is available, the mesh can be aligned with the image features by hand, and vertex colors can be automatically sampled from underlying pixels. A faster solution is to use optimisation techniques [21, 22] that optimize the color and position of vertices to best match the input image, as illustrated in Figure 1.9. Even if these methods are not entirely automatic, they save a lot of time for artists.

Alternative structures that work with triangular meshes for instance are a lot harder to draw entirely from scratch: the overall structure has to be changed when one wants to add details or move some parts of the structure. This is why such methods have been rather confined to automatic conversion.

When working with gradient extrema such as diffusion curves, a simple strategy consists of first drawing the curves as a line drawing, and then adding or editing colors and blur transitions along each curve. This approach is somewhat similar to the traditional "sketching + coloring" process in traditional drawing. Because of their flexibility, extremal primitives are also well adapted to multi-touch user interfaces [23]. To facilitate color editing, Jeschke et al. [13] propose storing for each pixel a list of the most influential curves and color control points. Users can then specify the color at a pixel to modify the color of the curves accordingly.

When a reference image is available, active contours [15] can be used to snap extremal curves to image locations where the color gradient is strong [19]. To assign color values, two methods have been proposed. A direct solution consists in sampling a dense set of color control points along each side of a curve directly from the image, and then simplifying the set of samples by keeping only the most relevant ones using the Douglas-Pucker algorithm [19]. However, this method still requires many color control points to reach satisfying results. A better solution, proposed by Jeschke et al. [13], consists in finding optimal color control points using a least-squares approach.

6.3.2 Automatic conversion

The earliest of automatic conversion methods were designed for image compression purposes, and relied on simple triangulations [6]. One of the first techniques that presented vectorization for stylization purposes is the Ardeco system [17] that converts bitmap images into linear or radial gradients. The core of this method is a region segmentation algorithm based on an energy minimization that combines two terms: one term aims at creating compact regions while the other term measures the goodness of fit of elemental color gradients.

As a result, the output of the system is a fully editable collection of 2D shapes with their assigned gradients, as illustrated in Figure 1.10. The method is particu-

(a) Input bitmap (b) Segmentation (c) Linear gradient approximation

Fig. 6.10 The Ardeco system [17] converts an input bitmap into a collection of linear or radial gradients. The algorithms segments the image into regions well approximated by the elemental gradients. ©Copyright 2006 Eurographics.

larly efficient at converting images of artwork composed of very smooth gradients and very sharp transitions, hence the name of the system which is reminiscent of the artistic movement of the twenties.

Although the restriction to elemental color gradients makes further editing straightforward, it also severely restricts the kind of images that can be depicted. Consequently, methods based on gradient meshes specifically tailored to image vectorization [16, 25] have flourished and greatly improved the accuracy of the conversion

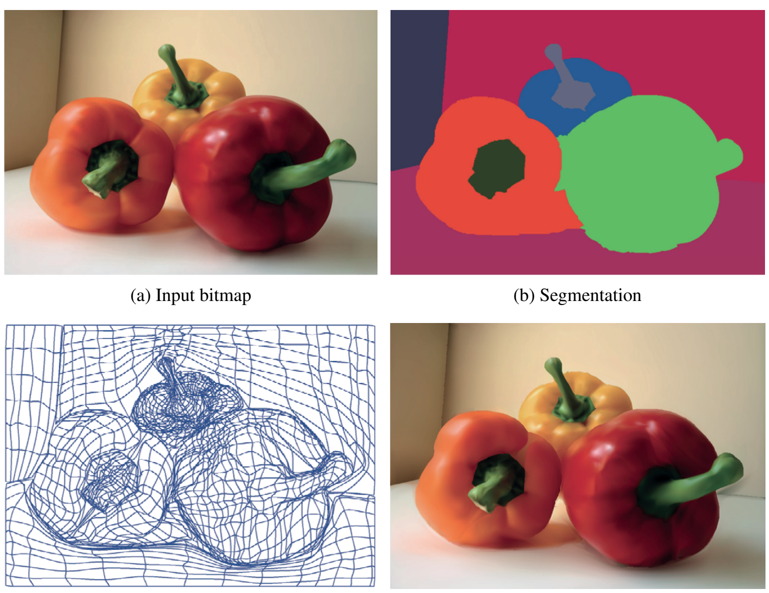

(a) Input bitmap (b) Segmentation

(c) Gradient meshes (d) Resulting image

Fig. 6.11 The method of Lai et al. [16] uses image segmentation to identify the main regions in the image. A gradient mesh is then optimized over each region. ©Copyright 2009 ACM.

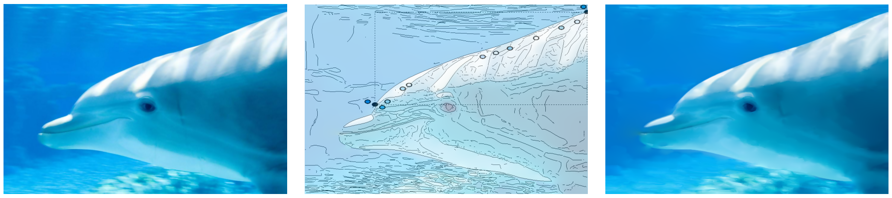

(a) Input bitmap (b) Vectorized edges with estimated color control points (c) Result after diffusion

Fig. 6.12 Automatic conversion of a bitmap image into diffusion curves. The algorithm fits Bezier splines on the image edges (b). Colors are sampled along each spline and approximated as polylines in color space. The resulting diffusion curve image closely matches the input bitmap, although details can be lost in textured regions. ©Copyright 2008 ACM.

process. Image segmentation and edge detection algorithms are typically used to identify the important features of the image and guide the mesh creation process, as illustrated in Figure 1.11.

Such methods produce images that can look remarkably similar to photographs, but are often difficult to edit and stylize due to the complexity of the resulting meshes. On the other hand, mesh-based representations are well suited to image deformations [1].

Edge detection algorithms can also be used to automate the conversion of bitmap images into gradient extrema. Elder and colleagues [7, 8] first proposed converting a bitmap image into a representation based on edges. However, their representation remains in a raster form suitable for image compression and editing. Orzan et al. [19] build upon this approach to vectorize diffusion curves with color and blur control points for stylization purposes. Their method works in two stages: 1) the bitmap image is analyzed at multiple scales to detect not only the most salient color edges, but also their blur which is important to represent out-of-focus objects or soft shadow boundaries; 2) the extracted data is converted to a vector form, in a way similar to methods for color assignment presented in the previous section.

An example is shown in Figure 1.12. Similar to the Ardeco system, results are easily edited using gradient extrema tools. In addition, gradient extrema are able to reproduce a greater variety of images (even photorealistic ones) with a small number of primitives, which makes their manipulation and editing more flexible than with mesh-based representations. However, representations based on gradient extrema reach their limits with textured images. By definition, textures contain a lot of edges, which prevent simple and direct editing. Very little work has been done on the vectorization of textured images with gradient extrema methods. A notable exception is the work of Jeschke et al. [13] that represent textures with procedural noise controlled by diffusion curves. Nevertheless, a challenging direction for future research is to generate the minimal set of extremal curves that vectorizes an image under a given quality threshold. This vectorization problem is related to image compression, although the measure of quality may also be designed to encourage the editability of the set of curves.

$$I_1(u,v) = vC_1(u) + (1\text{-}v)C_3(u)$$
$$I_2(u,v) = uC_2(v) + (1\text{-}u)C_4(v)$$
$$P(u,v) = (1\text{-}u)(1\text{-}v)P_{00} + (1\text{-}u)vP_{01} + u(1\text{-}v)P_{10} + uvP_{11}$$

$$I(u,v) = I_1(u,v) + I_2(u,v) - P(u,v)$$

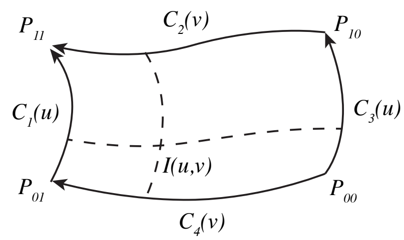

Fig. 6.13 A Coons patch is define by 4 vertices P_{00}, P_{01}, P_{11}, P_{10}, and is bounded by 4 curves $C_1(u)$, $C_2(v)$, $C_3(u)$, $C_4(v)$. The formula is used to interpolate the position and color of $I(u,v)$.

6.4 Rendering algorithms

Independently of the choice of primitive, the creation of an image requires a method to rasterize them into a grid of pixels. We make the distinction between methods that allow the computation of a pixel color from an analytical expression (closed-form methods) and methods that require solving a system of linear equations (optimization-based methods). Closed-form approaches allow the computation of pixels independently while optimization-based methods require computing the entire image at once.

6.4.1 Closed-form methods

Elemental gradients and gradient meshes are evaluated with closed-form methods, which makes them straightforward to render. For elemental gradients, rendering consists in a simple evaluation of Cartesian or polar coordinates, followed by a (usually linear) interpolation in the space of the 1D color gradient.

For gradient meshes, the first step consists in identifying to which patch P_i a pixel belongs to; then its parametric coordinates must be computed, and colors evaluated via a 2D interpolation.

The last step depends on the type of patch. In the common case of a regular quad-mesh, the color at the (u,v) coordinates of a patch is given by surface interpolation. Figure 1.13 provides the equations for the Coons patch to interpolate the position and color at a given coordinate (u,v) [9]. Sun et al. use the Ferguson patch for this purpose [22].

Due to the simplicity of the rendering process, these methods have found a widespread use in graphics applications. They have a limitation specific to rendering though: they do not deal with blurring in closed form. To compensate for this, some applications such as Inkscape rather apply a Gaussian blur in post-processing to produce more complex images.

6.4.2 Optimization-based methods

Methods based on gradient extrema define the color image as the solution to a partial-differential equation. The original formulation [19] uses the Laplace equation to enforce color variations in-between curves to be as smooth as possible. Finch et al. [10] propose instead to use the Bi-Laplace equation that provides higher-order smoothness.

The Laplace equation enforces an image to be as constant as possible by minimizing the Laplace operator, which is the sum of the second partial derivatives of the image I:

$$\Delta I(x,y) = \frac{\partial^2 I}{\partial x^2} + \frac{\partial^2 I}{\partial y^2} = 0. \tag{6.1}$$

A Diffusion Curve image is obtained by solving the Laplace equation subject to the color specified along the curves. To do so, Orzan et al. discretize the equation over the image grid using finite differences:

$$\begin{aligned} \Delta I(x,y) &= 4I(x,y) - \big(I(x-1,y) + I(x+1,y) + I(x,y-1) + I(x,y+1)\big) = 0 \\ I(x,y) &= C(x,y) \text{ if pixel } (x,y) \text{ stores a color value.} \end{aligned}$$

The resulting sparse linear system of equations can be solved with a direct solver, or using iterative solvers such as Jacobi relaxation that repeatedly update the value at a pixel from the values of neighboring pixels at the previous iteration:

$$\begin{aligned} I^{k+1}(x,y) &= \big(I^k(x-1,y) + I^k(x+1,y) + I^k(x,y-1) + I^k(x,y+1)\big)/4 \\ I^{k+1}(x,y) &= C(x,y) \text{ if pixel } (x,y) \text{ stores a color value.} \end{aligned}$$

To obtain real-time performances, Orzan et al. [19] adopt a multi-scale approach inspired by the multigrid algorithm [5] that applies Jacobi iterations in a coarse-to-fine scheme. Figure 1.14 illustrates this algorithm. The color constraints are first downsampled to form a pyramid. A few iterations on the coarsest level of the pyramid is sufficient to solve for the low frequencies of the image. This coarse solution is then repeatedly upsampled and refined to efficiently solve for the finer details in the image. Despite GPU implementations of the multigrid, the time to convergence may still be slow to generate images at high resolution. Jeschke et al. [12] present a faster solution that initializes the color at each pixel with the color of the closest curve, and uses finite differences with variable step size to accelerate the convergence rate of Jacobi iterations.

While the Laplace equation produces a smooth image away from color constraints, it does not enforce smooth derivatives. The resulting image is a membrane interpolant that forms creases, or "tents", along the diffusion curves. Finch et al. [10] provide smooth derivatives using the Bi-Laplace equation:

$$\Delta^2 I(x,y) = \left(\frac{\partial^2 I}{\partial x^2}\right)^2 + 2\left(\frac{\partial^2 I}{\partial xy}\right)^2 + \left(\frac{\partial^2 I}{\partial y^2}\right)^2 = 0, \tag{6.2}$$

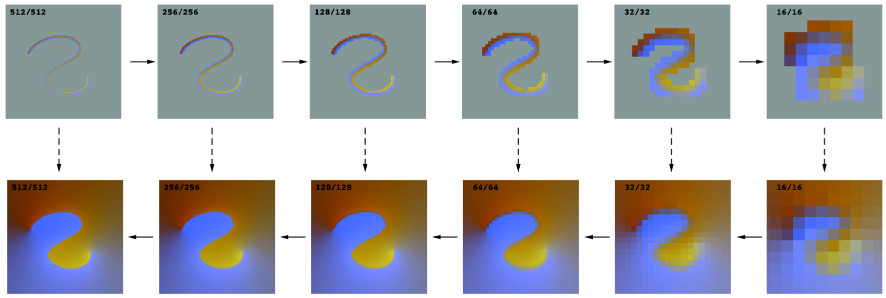

Fig. 6.14 The multigrid algorithm. Color constraints are repeatedly downsampled (top row). A coarse solution is quickly computed at the lowest level, by iteratively diffusing the color constraints. The solution is then upsampled and refined using the finer-scale color constraints (bottom row).

for which the solution is called the "Thin Plate Spline" function, a physical analogy involving the bending of a thin sheet of metal (see Figure 1.15). Using finite differences over the pixel grid, the discrete equation is expressed as:

$$\begin{aligned}\Delta^2 I(x,y) = {} & 20I(x,y) - 8\big(I(x-1,y)+I(x+1,y)+I(x,y-1)+I(x,y+1)\big)\\ & +2\big(I(x-1,y+1)+I(x+1,y+1)+I(x-1,y-1)+I(x+1,y-1)\big)\\ & +I(x-2,y)+I(x+2,y)+I(x,y-2)+I(x,y+2)=0\\ I(x,y) = {} & C(x,y) \text{ if pixel } (x,y) \text{ stores a color value.}\end{aligned}$$

As in Orzan et al. [19], Finch et al. use a multigrid solver to obtain the final color image. However, care must be taken when solving the linear system of equations because the Bi-Laplace problem has a larger condition number than the Laplace problem. A robust computation requires double-precision arithmetic, or damped iterative relaxations where the color of a pixel is only partly updated with the values of its neighbors at each iteration. Figure 1.15 provides a visual comparison between the solutions of the Laplace and Bi-Laplace equations.

These optimization techniques have a number of limitations in practice. When working with multigrid solvers, temporal flickering artifacts can occur when curves are edited because of the rasterization of the curves over a discrete multi-scale pixel grid. Although flickering is greatly reduced by the technique of Jeschke et al. [12], it only works for the original version of diffusion curves: extensions that have been further proposed are not trivial to render with an optimized solver. Moreover, although the thin plate spline solution is smoother than the membrane solution, it may produce unexpected colors as the thin plate splines can extrapolate colors while the membrane can only interpolate.

In all cases, important issues remain: the setting of color constraints on each side of a curve is prone to numerical inaccuracies when discretized on a pixel grid, and the blurring across a curve is usually performed by an additional diffusion of the blur values that control the size of a Gaussian blur applied in post processing.

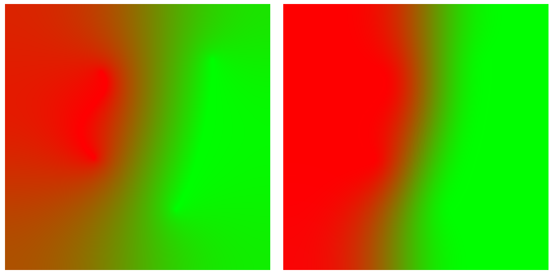

(a) Laplace equation (b) Bi-Laplace equation

Fig. 6.15 Comparison between the solution of the Laplace and Bi-Laplace equations. The Laplace equation produces a membrane interpolant with tent-like artifacts along the curves. The Bi-Laplace produces a thin-plate spline interpolant with higher smoothness.

6.4.3 Hybrid methods

Most of the limitations of optimisation-based solvers presented so far are due to one implicit assumption: that gradient extrema should be rasterized directly in a pixel grid. The methods we present in this section rather use an intermediate representation, which is then rasterized in a second step. Such hybrid methods are suitable for the fast rendering of static vector images, but any modification of the extremal curves requires re-building the intermediate representation.

Pang et al. [20] convert Diffusion Curves into a triangle-mesh representation where colors are linearly interpolated over each triangle. They first apply a constrained triangulation to build a mesh from the curves. The positive Mean-Value Coordinate (pMVC) interpolant is then used as a (closed-form) approximation to color diffusion in order to compute the color at each vertex of the mesh. In a nutshell, positive Mean-Value Coordinates expresses the interpolated color at a point as a weighted sum of the colors of the curves visible from this point. The main difficulty with this approach is to evaluate visibility efficiently. Pang et al. propose a sorting algorithm that identify the curve segments visible from each vertex. Similarly, Takayama et al. [24] use the hardware depth buffer to compute visibility of diffusion surfaces over the vertices of a mesh., while Bowers et al. [4] perform ray tracing in a pixel shader to render diffusion curves.

These methods have investigated a promising direction of research for rendering gradient extrema, with the potential practical effect of making these primitives available to a wider audience. However, they are still limited in a number of respects: none of them provides solutions to the Bi-Laplacian, and the approximations necessary for real-time rendering can degrade visual quality. Like previous rendering algorithms, blur is not dealt with directly, and should be added in post-processing.

Therefore, finding a propagation algorithm that combines the advantages of closed-form solutions with the flexibility of gradient extrema primitives remains a challenging research direction.

6.5 Discussion

We have presented vector primitives dedicated to the creation of color gradients, along with methods to construct them and algorithms to render images out of them. As of now, elemental gradients are ubiquitous in vector applications, and since gradient meshes have appeared in Adobe Illustrator, they have acquired support from a large base of users. However, only basic construction methods are available in vector graphics packages, and non-regular meshes are still confined to the vectorization of photographs. Diffusion Curves have appeared in various forms (standalone applications, webGL), but the issues raised by rendering algorithms makes it hard to run them on all platforms, since they often require advanced GPUs.

Gradient extrema are thus mainly limited regarding rendering, although in some instances it is easier to use gradient meshes because the control over interiors is more direct. On the other hand, gradient meshes are straightforward to render, but often tend to produce too dense representations. This tradeoff is reflected by the open scientific challenges we gave hints at throughout the chapter.

There might be a greater challenge though. To understand it, imagine placing the methods we have presented on an axis ranging from those more prone to creation, to those more adapted to conversion. Methods based on gradient extrema will cluster on the creation side, while those based on gradient meshes will rather be packed on the conversion side. In other words, there is a "virgin land" that has not yet been reached, and it might necessitate the invention of yet another kind of primitive, that better accounts for the structure found in images while still being sparse enough to promote direct, intuitive control.

Throughout this chapter we have only considered static images, but another appeal of vector graphics is animation. For instance, rotoscoping methods might make use of patches and curves to track image features from frame to frame and vectorize them. Then least-square optimizations could be employed to assign them colors smoothly in both space and time. Finally, these color gradients could serve as base layers to guide further stylization processes, hence finding their place in stylized rendering pipelines.

References

1. Barrett, W.A., Cheney, A.S.: Object-based image editing. ACM TOG (Proc. SIGGRAPH) **21**(3), 777–784 (2002). DOI 10.1145/566654.566651
2. Baxter, W.V., Scheib, V., Lin, M.C.: dAb: Interactive Haptic Painting With 3D Virtual Brushes. In: SIGGRAPH, pp. 461–468 (2001)
3. Bezerra, H., Eisemann, E., DeCarlo, D., Thollot, J.: Diffusion constraints for vector graphics. In: Proceedings of the International Symposium on Non-Photorealistic Animation and Rendering (NPAR), pp. 35–42 (2010). DOI 10.1145/1809939.1809944
4. Bowers, J.C., Leahey, J., Wang, R.: A Ray Tracing Approach to Diffusion Curves. Computer Graphics Forum (Proc. EGSR) **30**(4), 1345–1352 (2011). DOI 10.1111/j.1467-8659.2011.01994.x

5. Briggs, W.L., Henson, V.E., McCormick, S.F.: A multigrid tutorial. Society for Industrial and Applied Mathematics (2000)
6. Demaret, L., Dyn, N., Iske, A.: Image compression by linear splines over adaptive triangulations. Signal Process. **86**(7), 1604–1616 (2006). DOI 10.1016/j.sigpro.2005.09.003
7. Elder, J.H.: Are Edges Incomplete? Int. J. Comput. Vision **34**(2–3), 97–122 (1999). DOI 10.1023/A:1008183703117
8. Elder, J.H., Goldberg, R.M.: Image Editing in the Contour Domain. IEEE Trans. Pattern Anal. Mach. Intell. **23**(3), 291–296 (2001). DOI 10.1109/34.910881
9. Farin, G., Hansford, D.: Discrete Coons patches. Computer Aided Geometric Design **16**, 691–700 (1999)
10. Finch, M., Snyder, J., Hoppe, H.: Freeform vector graphics with controlled thin-plate splines. ACM Transactions on Graphics (Proc. SIGGRAPH Asia) **30**(6), 166:1–166:10 (2011). DOI 10.1145/2070781.2024200
11. Hnaidi, H., Guérin, E., Akkouche, S., Peytavie, A., Galin, E.: Feature based terrain generation using diffusion equation. Computer Graphics Forum (Proceedings of Pacific Graphics) **29**(7), 2179–2186 (2010)
12. Jeschke, S., Cline, D., Wonka, P.: A GPU Laplacian solver for diffusion curves and Poisson image editing. ACM Transactions on Graphics (Proc. SIGGRAPH Asia) **28**, 116:1–116:8 (2009). DOI 10.1145/1618452.1618462
13. Jeschke, S., Cline, D., Wonka, P.: Estimating Color and Texture Parameters for Vector Graphics. Computer Graphics Forum (Proc. Eurographics) **30**(2), 523–532 (2011)
14. Johnston, S.F.: Lumo: illumination for cel animation. In: Proceedings of the international symposium on Non-photorealistic animation and rendering (NPAR) (2002). DOI 10.1145/508530.508538
15. Kass, M., Witkin, A., Terzopoulos, D.: Snakes: Active contour models. International Journal of Computer Vision **1**(4), 321–331 (1988)
16. Lai, Y.K., Hu, S.M., Martin, R.R.: Automatic and topology-preserving gradient mesh generation for image vectorization. ACM Trans. Graph. **28**(3), 85:1–85:8 (2009). DOI 10.1145/1531326.1531391
17. Lecot, G., Lévy, B.: ARDECO: Automatic Region DEtection and Conversion. In: 17th Eurographics Symposium on Rendering - EGSR'06, pp. 349–360 (2006)
18. McCann, J., Pollard, N.S.: Real-Time Gradient-Domain Painting. ACM TOG (Proc. SIGGRAPH) **27**(3), 93:1–93:7 (2008)
19. Orzan, A., Bousseau, A., Winnemöller, H., Barla, P., Thollot, J., Salesin, D.: Diffusion curves: a vector representation for smooth-shaded images. ACM Transactions on Graphics (Proc. SIGGRAPH) **27**, 92:1–92:8 (2008). DOI http://doi.acm.org/10.1145/1360612.1360691
20. Pang, W.M., Qin, J., Cohen, M., Heng, P.A., Choi, K.S.: Fast Rendering of Diffusion Curves with Triangles. IEEE Computer Graphics and Applications **99**(PrePrints) (2011). DOI 10.1109/MCG.2011.86
21. Price, B.L., Barrett, W.A.: Object-based vectorization for interactive image editing. The Visual Computer **22**(9-11), 661–670 (2006). DOI 10.1007/s00371-006-0051-1
22. Sun, J., Liang, L., Wen, F., Shum, H.Y.: Image vectorization using optimized gradient meshes. ACM Trans. Graph. **26**(3) (2007). DOI 10.1145/1276377.1276391
23. Sun, Q., Fu, C.W., He, Y.: An interactive multi-touch sketching interface for diffusion curves. In: Proceedings of the 2011 annual conference on Human factors in computing systems (CHI), pp. 1611–1614 (2011). DOI 10.1145/1978942.1979176
24. Takayama, K., Sorkine, O., Nealen, A., Igarashi, T.: Volumetric modeling with diffusion surfaces. ACM Transactions on Graphics (Proc. SIGGRAPH Asia) **29**, 180:1–180:8 (2010). DOI 10.1145/1882261.1866202
25. Xia, T., Liao, B., Yu, Y.: Patch-based image vectorization with automatic curvilinear feature alignment. ACM Trans. Graph. **28**(5), 115:1–115:10 (2009). DOI 10.1145/1618452.1618461